

A Novel Electronic-continuously Variable Transmission Propulsion System Using Coaxial Magnetic Gearing for Hybrid Electric Vehicles

Linni Jian¹ and K. T. Chau²

¹ Department of Electrical and Electronic Engineering, The University of Hong Kong, lnjian@eee.hku.hk

² Department of Electrical and Electronic Engineering, The University of Hong Kong, ktchau@eee.hku.hk

Abstract

As one of the most attractive technologies for hybrid electric vehicles, the electronic-continuously variable transmission (E-CVT) propulsion system has received more and more attention. In this paper, a novel E-CVT propulsion system using coaxial magnetic gearing is proposed. It can achieve optimal fuel economy, minimum exhaust emission as well as good propulsion performance by flexibly distributing the power flows. Since the coaxial magnetic gearing can offer non-contact torque transmission, the drawbacks of low transmission efficiency, mechanical friction and audible noise aroused from the mechanical planetary gearing can be overcome. The connection topology and the operation modes of the proposed system are analyzed and discussed.

Keywords

coaxial magnetic gear, hybrid electric vehicles, electric variable transmission, permanent magnet machine

1. INTRODUCTION

With ever increasing concerns on energy crisis and global warming, there is fast-growing interest in hybrid electric vehicles (HEVs) [Wong et al., 2005; Wong et al., 2006; Chau and Chan, 2007]. At present, one of the most attractive technologies for HEVs is the electronic-continuously variable transmission (E-CVT) propulsion system, which involves two mechanical ports and two electrical ports [Miller, 2006]. By flexibly distributing the power flow among the internal combustion engine (ICE), the final driveline (FD) and the electrical sources, the E-CVT propulsion system can achieve optimal fuel economy, minimum gas emission and good propulsion performance.

In order to realize flexible distribution of the power flow among several power paths, a junction device which can offer multi-port power transmission is indispensable. In the existing E-CVT propulsion systems, such as the Toyota E-CVT and Ford E-CVT [Miller and Everett, 2005], a planetary gear set is usually employed to play this role. However, it suffers from the drawbacks of low transmission efficiency, significant mechanical friction and annoying audible noise. Recently, several types of concentrically arranged double-rotor electric machine for E-CVT propulsion have also been proposed [Hoeijmakers and Ferreira, 2006; Chau et al., 2008]. Nevertheless, they need carbon brushes and slip rings to withdraw power from the primary rotor. With no doubt, this will deteriorate the reliability of the whole system. Very

recently, a high performance coaxial magnetic gearing (CMG) device has been proposed [Atallah and Howe, 2001; Chau et al., 2008; Jian and Chau, 2009a]. It can provide non-contact torque transmission and speed variation using the modulation effect of permanent magnet fields. Hence, the drawbacks of transmission efficiency, mechanical friction and audible noise brought by the mechanical gearing can be avoided. It also has been successfully applied to direct-drive wind power generators [Jian et al., 2009] and in-wheel motors [Chau et al., 2007; Jian and Chau, 2009b].

The purpose of this paper is to propose a novel E-CVT propulsion system using CMG, in which two permanent magnet (PM) machines are integrated with a CMG to achieve high-performance power flow splitting and mixing for the HEVs. In section 2, the system configuration will be introduced. Section 3 will be devoted to the analysis of operation modes. Finally, conclusion will be drawn in section 4.

2. SYSTEM CONFIGURATION

2.1 CMG offering continuously variable speed transmission

Figure 1 shows the topology of the CMG. It employs high-energy rare-earth PMs on both the inner rotor and the outer rotor, and has the modulating ring sandwiched between the two rotors. The modulating ring takes charge of modulating the magnetic fields in two airgaps beside it. In order to form good magnetic paths as well as to reduce eddy current loss, the modulating ring is built of thin sheets of laminated ferromagnetic materials. Also, epoxy is filled in its slots to enforce the structural strength for high torque transmission. By defining the p_1 and p_2 as the pole-pair numbers of

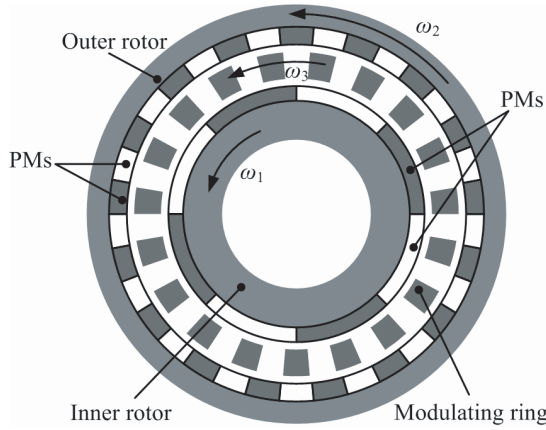


Fig. 1 Topology of coaxial magnetic gear

the inner and outer rotors, respectively, and n_s as the number of ferromagnetic segments on the modulation ring, the CMG can achieve stable torque transmission only if it satisfies:

$$n_s = p_1 + p_2 \quad (1)$$

When the modulating ring is fabricated as a stationary component, the CMG can offer fixed-ratio variable speed transmission, and the corresponding speed relationship can be expressed as:

$$\omega_1 = -\frac{p_2}{p_1} \omega_2 = -G_r \omega_2 \quad (2)$$

where ω_1 , ω_2 are the rotational speeds of the outer rotor and inner rotor respectively, G_r is the so-called gear ratio, and the minus sign indicates that the two rotors rotate in opposite directions.

In order to achieve multi-port power flow distribution, herein, the modulating ring is designed as another rotational part. Thus the CMG can offer continuously variable speed transmission, and the corresponding speed relationship is governed by:

$$\omega_1 + G_r \omega_2 - (1 + G_r) \omega_3 = 0 \quad (3)$$

where ω_3 is the rotational speeds of the modulating ring. Without considering the power losses occurred in the CMG, it yields:

$$T_1 \omega_1 + T_2 \omega_2 + T_3 \omega_3 = 0 \quad (4)$$

$$T_1 + T_2 + T_3 = 0 \quad (5)$$

where T_1 , T_2 and T_3 are the developed magnetic torques on the inner rotor, the outer rotor and the modulating ring, respectively.

2.2 E-CVT propulsion systems using CMG

Generally, the working point of a vehicle is changing frequently and fiercely in driving, which means the output speed and torque of the FD is adjusted from time to time according to the external factors such as the road conditions and the driver's behavior. However, as shown in Figure 2, there is a unique optimal operating line (OOL) for each ICE, on which, it can work with the maximum fuel economy and the minimum exhaust emission. For this reason, the E-CVT propulsion system dynamically distributes the power flow among the ICE, the FD and the DC source by using two machines, hence to satisfy the demands of the FD and keep the ICE working on the OOL simultaneously. As a junction device, the aforementioned CMG can offer three rotational mechanical ports. Thus, how to connect the FD, the ICE and the machines to these mechanical ports becomes an essential problem when designing the E-CVT propulsion system. Figure 3

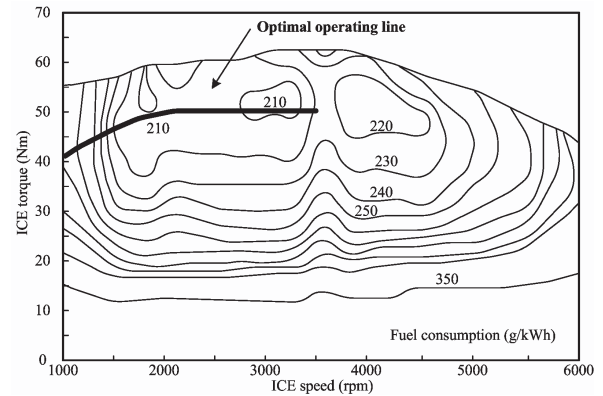


Fig. 2 ICE optimal operating line

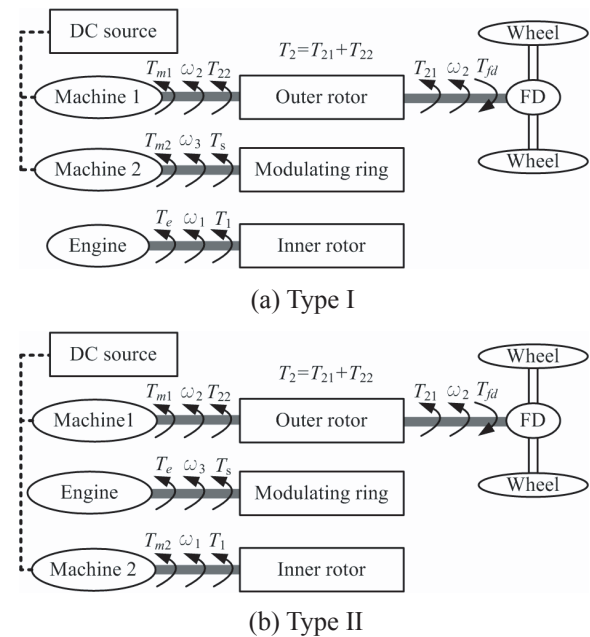


Fig. 3 Possible connections for E-CVT

depicts two possible connections. Figure 3(a) shows the type I, in which the machine 1 and the FD shaft are attached to the outer rotor, the machine 2 is connected to the modulating ring and the engine shaft is attached to the inner rotor. Figure 3(b) shows the type II, in which the machine 1 and the FD shaft are also attached to the outer rotor, the machine 2 is connected to the inner rotor and the engine shaft is attached to the modulating ring.

Apart from the (1)-(5), the system dynamics are governed by:

$$T_2 = T_{21} + T_{22} \quad (6)$$

$$T_{21} - T_{fd} = J_{fd} \frac{d\omega_2}{dt} \quad (7)$$

$$T_{22} + T_{m1} = J_{m1} \frac{d\omega_2}{dt} \quad (8)$$

$$T_3 + T_{m2} = J_3 \frac{d\omega_3}{dt} \quad (9)$$

$$T_e + T_1 = J_1 \frac{d\omega_1}{dt} \quad (10)$$

$$T_1 + T_{m2} = J_1 \frac{d\omega_1}{dt} \quad (11)$$

$$T_e + T_3 = J_3 \frac{d\omega_3}{dt} \quad (12)$$

where (9) and (10) are limited to the type I whereas (11) and (12) are limited to the type II; J_{fd} , J_{m1} , J_{m2} , J_1 , J_2 , J_3 are the moments of inertia of FD shaft, rotor of machine 1, rotor of machine 2, inner rotor of CMG, outer rotor of CMG and modulating ring of CMG, respectively; T_{fd} , T_{m1} , T_{m2} , T_{21} , T_{22} are the load torque of FD, output torque of machine 1, output torque of machine 2, the component of T_2 on the FD shaft, the component of T_2 on the rotor shaft of machine 1, respectively.

For each type of connection, the directions of the ICE shaft and the FD shaft can be designed with the same direction or the opposite directions. There are four possible cases:

- Case 1: the connection type I is adopted and the directions of the ICE shaft (ω_1) and the FD shaft (ω_2) are designed with the same direction.
- Case 2: the connection type I is adopted and the directions of the ICE shaft (ω_1) and the FD shaft (ω_2) are designed with the opposite directions.
- Case 3: the connection type II is adopted and the directions of the ICE shaft (ω_3) and the FD shaft (ω_2) are designed with the same direction.
- Case 4: the connection type II is adopted and the directions of the ICE shaft (ω_3) and the FD shaft

(ω_2) are designed with the opposite directions.

As mentioned above, the goal of the E-CVT propulsion system is to satisfy the demands of the FD and keep the ICE working on the OOL simultaneously. For simplicity, a sole optimum working point is chosen for the ICE, and different working points of the FD are considered. Figure 4 gives the chosen optimum working point O (3000 rpm, 50 Nm) for the ICE and six typical working points for the FD, namely, A (500 rpm, 320 Nm), B (700 rpm, 210 Nm), C (900 rpm, 190 Nm), D (1100 rpm, 130 Nm), E (1300 rpm, 100 Nm) and F (1500 rpm, 80 Nm). The corresponding power of each point is also illustrated in Figure 4. It can be seen that for the working points A and C , the DC source will assist the ICE to supply power to the FD via the machines, and for the working points B , D , E and F , the ICE will charge the DC sources with the redundant power via the machines.

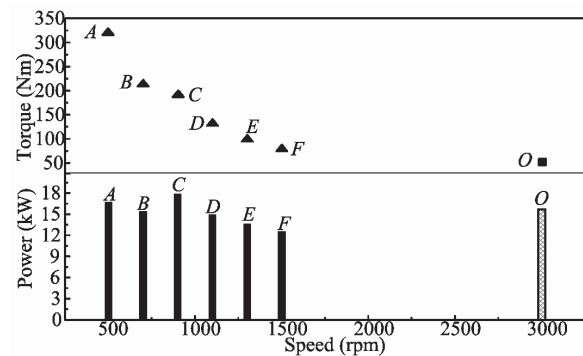
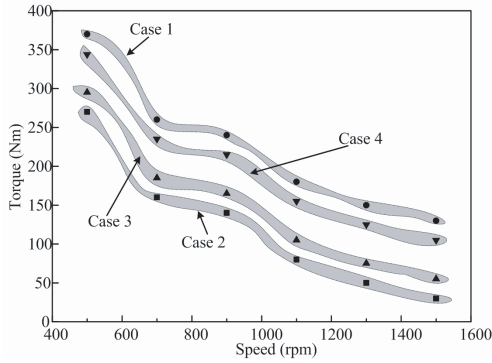
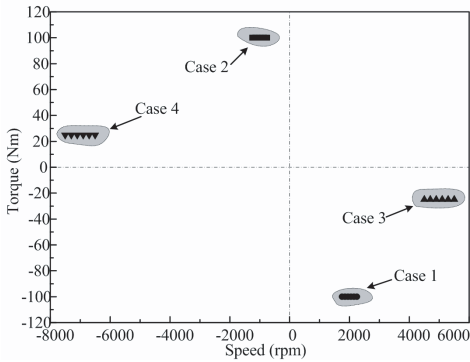


Fig. 4 Working points of finial driveline considered

According to (2)-(12), the working points of the two machines can be calculated under different working points of the FD and the optimum working point of the ICE. Consequently, the results with different gear ratio G_r are illustrated in Figures. 5, 6 and 7. It can be found that in the cases 1 and 2, the machine 2 works at high torque and very low speed (sometimes even zero), which means that the machine 2 has to be designed with bulky size and high current rating, which are unattractive for HEV application. In contrast, in the cases 3 and 4, the machine 2 works in the low torque and high speed range which is helpful for designing a machine with light weight and small size, thus satisfying the demand of the HEV application. Comparing the case 3 and case 4, it is easy to observe that the case 3 is more preferable, since the machine 1 in the case 3 has much lower working torque than that in the case 4, and the working speed of machine 2 in the case 3 is more suitable than that in the case 4. Referring to the gear ratio, the bigger G_r implies lower working torque and higher working speed of machine 2. For practical application, the $G_r = 2$ is a proper choice.

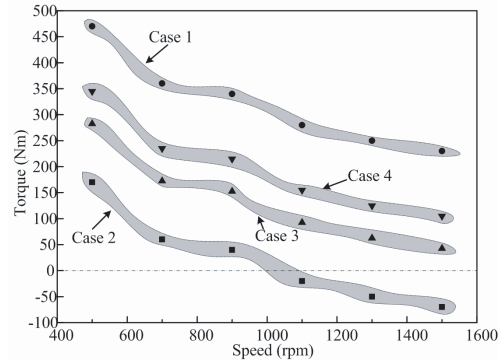


(a) Machine 1

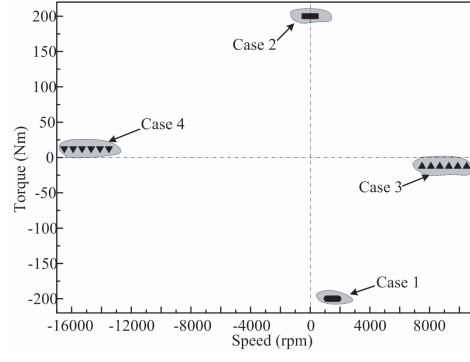


(b) Machine 2

Fig. 5 Distribution of working points of machines with $G_r=1$

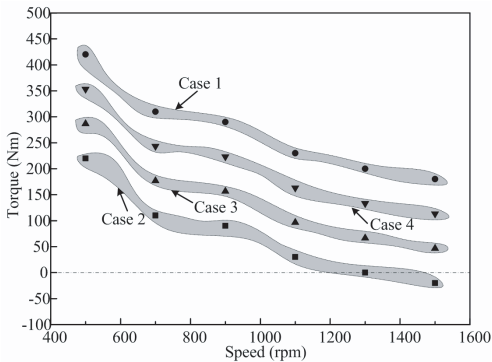


(a) Machine 1

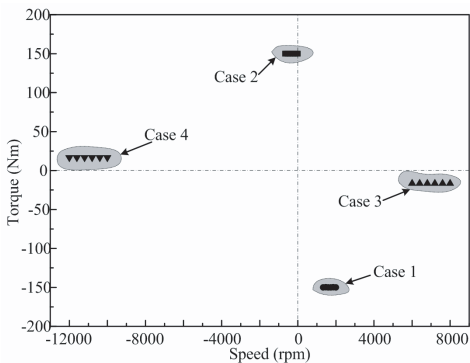


(b) Machine 2

Fig. 7 Distribution of working points of machines with $G_r=3$



(a) Machine 1



(b) Machine 2

Fig. 6 Distribution of working points of machines with $G_r=2$

Consequently, the topology of the proposed E-CVT propulsion system is shown in Figure 8. It integrates a CMG and two machines. With the CMG, the inner rotor is attached to the rotor of the machine 2, the modulating ring is connected to the ICE shaft, and the outer rotor which is also the rotor of the machine 1 is attached to the FD shaft. The armature windings of the two machines are connected to the DC source (battery or ultracapacitor bank) via two converters to enable the bidirectional power flow.

3. OPERATION MODES

3.1 Full-electric mode

In some cases, such as mild launching and low-speed crawling, both the demands of the output torque and rotational speed of the FD are quite low. If the battery state of charge (SOC) is high enough, the central control unit (CCU) will turn off the ICE to avoid its low efficiency operation, and the vehicle enters into the full-electric mode. In this mode, since the ICE is off, the modulating ring is always kept still, and the CMG works as a fixed-ratio gear. Thus the vehicle can be solely propelled by the machine 2. Once the demand of output torque of the FD exceeds the capability of the machine 2, the CCU will turn on the machine 1 to offer assistance.

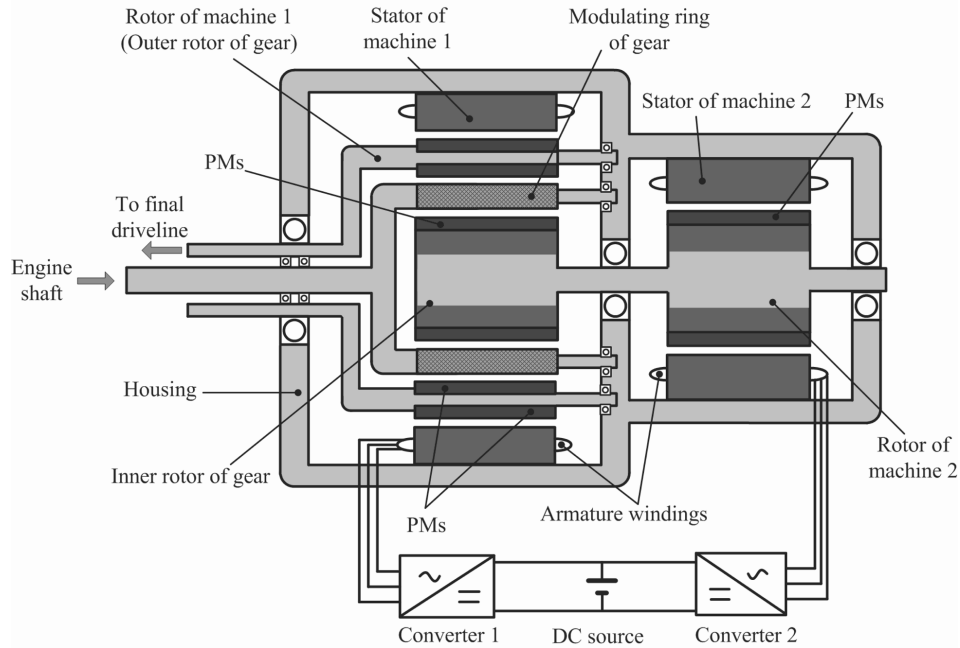


Fig. 8 Topology of proposed E-CVT propulsion system

3.2 Hybrid mode

In this mode, the ICE and the machines are working together. The CCU dynamically distributes the power flows aiming at the following three goals: (1) satisfy the demand of the FD; (2) keep the ICE working on the OOL; (3) keep the SOC of batteries at the rated level. The control block diagram of the CCU is illustrated by Figure 9. Firstly, the output torque and power demand of the FD is calculated according to the accelerator pressure, brake pressure and vehicle speed. Then, the throttle angle reference α^* of the ICE is obtained according to the OOL, and the adopted throttle angle is decided by the SOC of the battery. Namely, if the SOC level is lower than its rated value,

the adopted throttle angle should be increased by $\Delta\alpha$, and the redundant power offered by the ICE is used to charge the batteries. Otherwise, if the SOC level is higher than its rated value, the adopted throttle angle should be decreased by $\Delta\alpha$, and the batteries will offer positive power to assist the ICE. Next, the working points of the ICE and the two machines can be determined. Finally, the entire reference signals are fed into the machine controller to generate switching signals for the converters.

4. CONCLUSION

In this paper, a novel E-CVT propulsion system using CMG has been proposed for HEVs. It can achieve

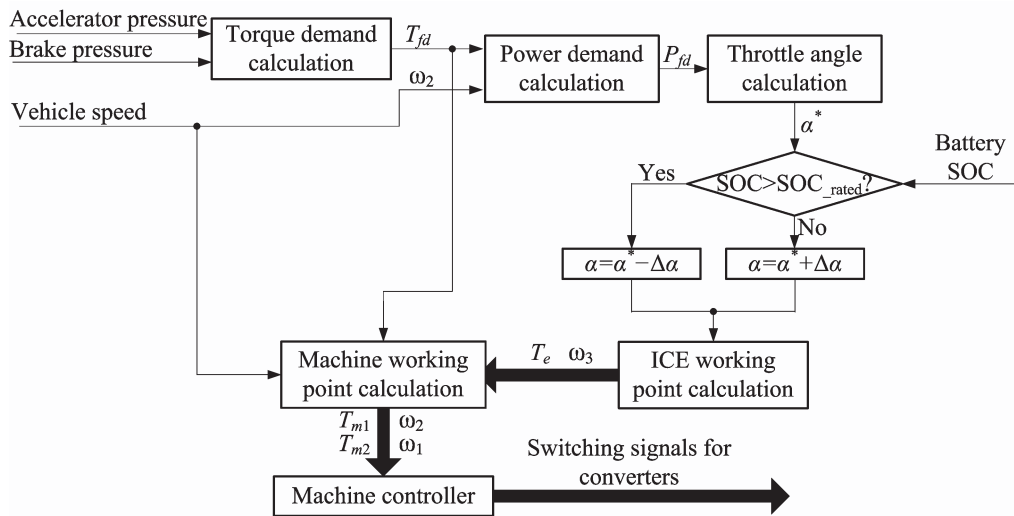


Fig. 9 Control block diagram of central control unit

optimal fuel economy, minimum exhaust emission as well as good propulsion performance by flexibly distributing the power flows. Since the CMG can offer non-contact torque transmission, the drawbacks of low transmission efficiency, significant mechanical friction and annoying audible noise aroused from the mechanical planetary gearing can be overcome. The connection topology and the operation modes of the system have been analyzed and discussed.

Acknowledgements

This work was supported by a grant (HKU 7105/07E) from the Research Grants Council, Hong Kong Special Administrative Region, China.

References

- Atallah, K., and D. Howe, A novel high performance magnetic gear, *IEEE Transactions on Magnetics*, Vol. 37, No. 4, 2844-2846, 2001.
- Chau, K. T., and C. C. Chan, Emerging energy-efficient technologies for hybrid electric vehicles, *Proceeding of IEEE*, Vol. 95, No. 4, 821-835, 2007.
- Chau, K. T., C. C. Chan, and C. Liu, Overview of permanent-magnet brushless drives for electric and hybrid electric vehicles, *IEEE Transactions on Industry Electronics*, Vol. 55, No. 6, 2246-2257, 2008.
- Chau, K. T., D. Zhang, J. Z. Jiang, and L. Jian, Transient analysis of coaxial magnetic gears using finite element comodeling, *Journal of Applied Physics*, Vol. 103, No. 7, 1-3, 2008.
- Chau, K. T., D. Zhang, J. Z. Jiang, C. Liu, and Y. J. Zhang, Design of a magnetic-gear outer-rotor permanent-magnet brushless motor for electric vehicles, *IEEE Transactions on Magnetics*, Vol. 43, No. 6, 2504-2506, 2007.
- Hoeijmakers, M. J., and J. A. Ferreira, The electric variable transmission, *IEEE Transactions on Industry Applications*, Vol. 42, No. 4, 1092-1100, 2006.
- Jian, L., and K. T. Chau, Analytical calculation of magnetic field distribution in coaxial magnetic gears, *Progress in Electromagnetics Research*, Vol. 92, 1-16, 2009a.
- Jian, L., and K. T. Chau, Design and analysis of an integrated halbach-magnetic-gear permanent-magnet motor for electric vehicles, *Journal of Asian Electric Vehicles*, Vol. 7, No. 1, 1213-1219, 2009b.
- Jian, L., K. T. Chau, and J. Jiang, A magnetic-gear outer-rotor permanent-magnet brushless machine for wind power generation, *IEEE Transactions on Industry Applications*, Vol. 45, No.3, 954-962, 2009.
- Miller, J. M., and M. Everett, An assessment of ultra-

capacitors as the power cache in Toyota HTS-II, GM-allision AHS-2 and Ford FHS hybrid propulsion systems, *Proceeding of 20th Annual Applied Power Electronics Conference Exposition*, Vol. 1, 481-490, 2005.

Miller, J. M., Hybrid electric vehicle propulsion system architectures of the E-CVT type, *IEEE Transactions on Power Electronics*, Vol. 21, No. 3, 756-767, 2006.

Wong, Y. S., K. T. Chau, and C. C. Chan, Battery sizing for plug-in hybrid electric vehicles, *Journal of Asian Electric Vehicles*, Vol. 4, No. 2, 899-904, 2006.

Wong, Y. S., K. T. Chau, and C. C. Chan, Load forecasting of hybrid electric vehicles under real time pricing, *Journal of Asian Electric Vehicles*, Vol. 3, No. 2, 815-818, 2005.

(Received August 2, 2009; accepted September 21, 2009)